REPORT

De novo stop-loss variants in *CLDN11* cause hypomyelinating leukodystrophy

Korbinian M. Riedhammer,[1,2] Sylvia Stockler,[3] Rafal Ploski,[4] Maren Wenzel,[5] Burkhard Adis-Dutschmann,[6] Uwe Ahting,[1] Bader Alhaddad,[1] Astrid Blaschek,[7] Tobias B. Haack,[1,8] Robert Kopajtich,[1,9] Jessica Y. Lee,[10] Victor Murcia Pienkowski,[4] Agnieszka Pollak,[4] Krystyna Szymanska,[11] Robin van der Lee,[10] Clara D. van Karnebeek,[10,12] Thomas Meitinger,[1] Ingeborg Krägeloh-Mann[13] and Katharina Vill[7]

Claudin-11, a tight junction protein, is indispensable in the formation of the radial component of myelin. Here, we report *de novo* stop-loss variants in the gene encoding claudin-11, *CLDN11*, in three unrelated individuals presenting with an early-onset spastic movement disorder, expressive speech disorder and eye abnormalities including hypermetropia. Brain MRI showed a myelin deficit with a discrepancy between T_1-weighted and T_2-weighted images and some progress in myelination especially involving the central and peripheral white matter. Exome sequencing identified heterozygous stop-loss variants c.622T>C, p.(*208Glnext*39) in two individuals and c.622T>G, p.(*208Gluext*39) in one individual, all occurring *de novo*. At the RNA level, the variant c.622T>C did not lead to a loss of expression in fibroblasts, indicating this transcript is not subject to nonsense-mediated decay and most likely translated into an extended protein. Extended claudin-11 is predicted to form an alpha helix not incorporated into the cytoplasmic membrane, possibly perturbing its interaction with intracellular proteins. Our observations suggest that stop-loss variants in *CLDN11* expand the genetically heterogeneous spectrum of hypomyelinating leukodystrophies.

1 Institute of Human Genetics, Klinikum rechts der Isar, School of Medicine, Technical University of Munich, Munich, 81675, Germany
2 Department of Nephrology, Klinikum rechts der Isar, School of Medicine, Technical University of Munich, Munich, 81675, Germany
3 Division of Biochemical Diseases, Department of Pediatrics, B.C. Children's Hospital, The University of British Columbia, Vancouver, BC V6H 0B3, Canada
4 Department of Medical Genetics, Medical University of Warsaw, Warsaw, 02-106, Poland
5 Genetikum, Genetic Counseling and Diagnostics, Neu-Ulm, 89231, Germany
6 Center for Pediatrics, Ulm, 89073, Germany
7 Dr. v. Hauner Children's Hospital, Department of Pediatric Neurology and Developmental Medicine, LMU – University of Munich, 80337, Germany
8 Institute of Medical Genetics and Applied Genomics, University of Tübingen, 72076 Tübingen, Germany
9 Institute of Neurogenomics, Helmholtz Zentrum München, German Research Center for Environmental Health, Neuherberg, 85764, Germany
10 Centre for Molecular Medicine and Therapeutics, BC Children's Hospital Research Institute, Department of Medical Genetics and Pediatrics, The University of British Columbia, Vancouver, BC V6H 0B3, Canada
11 Department of Experimental and Clinical Neuropathology, Mossakowski Medical Research Center, Polish Academy of Sciences, Warsaw, 02-106, Poland
12 Department of Pediatric Metabolic Diseases, Amalia Children's Hospital, Radboud University Medical centre, Nijmegen, 6525 GA, The Netherlands
13 Department of Pediatric Neurology and Developmental Medicine, University Children's Hospital, Tübingen, 72076, Germany

Correspondence to: Korbinian M. Riedhammer, MD
Institute of Human Genetics
Klinikum rechts der Isar
Technical University of Munich
Trogerstr. 32
81675 Munich
Germany
E-mail korbinian.riedhammer@mri.tum.de

Introduction

Impaired development of myelin is the hallmark of hypomyelinating leukodystrophies, a group of genetically heterogeneous disorders (Pouwels *et al.*, 2014). MRI led to the delineation of distinct disease entities around 15 years ago. As a result of the development of new methods of molecular genetic testing, the number of genetically defined leukodystrophies has increased in recent years (van der Knaap *et al.*, 2019). Since the association of variants in *PLP1* with Pelizaeus-Merzbacher disease [PMD (MIM 312080)], more than 10 different hypomyelinating leukodystrophies with more or less characteristic clinical features, such as 4H leukodystrophy, have been described and received a sequential 'HLD-' number in OMIM (Vanderver *et al.*, 2015). Increasing knowledge on the diversity of white matter pathology underlying leukodystrophies confirms that all its constituents determine white matter integrity and function. In the past decade, it became evident that not only variants in genes encoding structural oligodendrocyte proteins may be involved in hypomyelination leukodystrophies, but also variants in genes coding for transcription factors controlling expression of structural genes as well as variants in other genes with cellular roles less obviously linked with oligodendrocyte function (van der Knaap and Bugiani, 2018).

The correct formation of myelin plays a pivotal role in proper function of the CNS. The myelin sheath is assembled in multiple layers of lipid-rich membranes encasing the axon. This sheath is crucial for saltatory conduction along axons allowing the emergence of action potentials only at the nodes of Ranvier (Denninger *et al.*, 2015). The principal component of myelin integrity in the CNS is proteolipid protein (PLP), a lipid-associated tetraspan protein that is widely expressed in oligodendrocytes (Luders *et al.*, 2019). Tight junctions are further important elements of the myelin sheath. They structure the radial component of myelin and act as diffusion barriers. Claudin-11 (*CLDN11*, 3q26.2), a tetraspan protein like PLP and a member of the claudin tight junction family, is an indispensable part of the radial component of myelin (Denninger *et al.*, 2015).

Here, we describe three unrelated individuals with a hypomyelinating leukodystrophy, in whom exome sequencing detected heterozygous *de novo* stop-loss variants in *CLDN11*.

Materials and methods

Consent

Written informed consent for sequencing and publication in a scientific journal was obtained by the legal guardians of all three individuals according to the Declaration of Helsinki and this study has been approved by the ethical committees of the respective institutions in Munich, Warsaw and Vancouver.

Next-generation sequencing

Trio exome sequencing (exome sequencing of index and parents) was performed in Individuals 1 and 3. Proband-only exome sequencing with subsequent targeted-sequencing of the *CLDN11* stop-loss variant in the parents was performed in Individual 2 (see Supplementary material for further details).

RNA sequencing

RNA from fibroblasts was sequenced as described in Kremer *et al.* (2017) but as strand-specific mRNA according to the TruSeq Stranded mRNA Sample Prep Guide on a NovaSeq 6000 platform (Illumina) (Kremer *et al.*, 2017). Next, RNA sequencing data were analysed to detect differentially expressed genes compared to 156 control fibroblasts (Supplementary material).

Protein visualization and modelling

The protein sequence of extended claudin-11 was visualized using the free web-based tool Protter (http://wlab.ethz.ch/protter/start/) (Omasits *et al.*, 2014). Modelling of tertiary structure of added amino acids was done with PEP-FOLD and cytoplasmic localization of added amino acids was predicted with TMHMM (all for variant c.622T>C) (Krogh *et al.*, 2001; Thevenet *et al.*, 2012; Shen *et al.*, 2014).

Cranial MRI interpretation

MRIs were analysed visually and described with respect to myelin specific changes. For standardized evaluation of myelination, T_2-weighted images were scored with a semiquantitative myelination score with a maximum score of 36 characterizing complete myelination (Plecko *et al.*, 2003).

Data availability

All data can be shared. Results from molecular genetic analysis and RNA sequencing are available at the authors' institutions in Munich, Warsaw and Vancouver.

Results

Clinical synopsis

All three affected individuals were of non-Finnish European descent.

In Individual 1 (female), spasticity predominantly of the lower limbs and truncal hypotonia became apparent in the first year of life. Walking independently never exceeded a few metres and she had knee and ankle contractures. She presented with nystagmus, a hyperopic astigmatism of +2 dpt and strabismus, surgically treated at the age of 3 years.

Individual 2 (male) showed first signs of spasticity of all extremities with truncal hypotonia at the age of 4 months. Over time he developed muscular rigidity in the trunk, shoulder girdle and in the upper extremities. Walking without help became possible only over a couple months at the age of 5 years. He showed oral hypotonia with severe drooling and presented with nystagmus, early-onset strabismus (apparent already at age 4 months), which was multiply surgically treated, and hypermetropia of +4.5/+4.25 dpt (at age 8 years).

In Individual 3 (male), a spastic movement disorder with increased tone of the extremities (pronounced in the lower extremities), arching of neck, and plagiocephalus, became apparent at age 11 months. Walking without help was never achieved. He had oral hypotonia with constant drooling and presented with strabism with exotropic eye alignment, a fine nystagmus, decreased visual acuity near and far and a hyperopic astigmatism +3.25 dpt OD and +2.75 dpt OS.

All showed a pronounced delay in speech development, reached the ability to speak in sentences, but were all severely dysarthric. IQ was not tested in any of them, but intellectual disability seems to be mild at most. Hearing was unaffected in all and no involvement of internal organs occurred in any.

Electrophysiology revealed disturbed sensory evoked potentials in individual 1 (not performed in Individuals 2 and 3). Peripheral nerve conduction studies were normal in all three.

Broad diagnostic work-up included genetic and metabolic tests in all individuals, which remained without any indicative findings despite repeatedly elevated blood lactate in Individual 3 (2.3–6.1 mmol/l).

Table 1 provides geno- and phenotypic characteristics of the three individuals. Extended case reports are provided as case reports in the Supplementary material. See also Supplementary Video 1 for Individual 1.

Neuroimaging

In Individual 1, MRI of the brain was performed at the age of 14 months and 3.25 years, and showed clear characteristics of hypomyelination with a discrepancy between T_1-weighted and T_2-weighted images but with some progress in myelination over time. T_1-weighted images showed signal hyperintensity near to normal for age with respect to structures involved. T_2-weighted images, however, did not demonstrate relevant myelination of white matter structures (signal hypointensity) at 14 months; at 3.25 years, the cerebellar white matter had a hypointense signal, and mild hypointensity was seen in the corpus callosum, the posterior limb of the internal capsule (PLIC), as well as the frontal and occipital central white matter; myelination scores were 7 and 13, respectively. Individual 1 is the only individual showing some atrophy of the telencephalon on follow-up MRI.

In Individual 2, MRI scans were done at 7 months, 3.5 years, 4.3 years, and 6 years, which showed hypomyelination with characteristics similar to Individual 1. Over the years, some progress in myelination could be seen especially in central and even peripheral white matter, but not in the PLIC or periventricular white matter. Myelination scores were 4, 8, 10 and 14.

In Individual 3, MRIs were performed at age 16 months and 3.75 years and showed hypomyelination comparable to Individuals 1 and 2, also with some progress in myelination especially involving the central and peripheral white matter. Myelination scores were 7 and 16, respectively (Fig. 1).

Molecular genetic analysis and protein prediction

No disease-causing variant(s) in known disease-associated genes could be identified by exome sequencing in Individuals 1–3.

Trio exome sequencing of Individual 1 at 12 years of age revealed a heterozygous de novo stop-loss variant in CLDN11 NM_005602.5:c.622T>C, p.(*208Glnext*39).

Proband-only exome sequencing of Individual 2 at 7 years of age revealed a heterozygous stop-loss variant in CLDN11 NM_005602.5:c.622T>G, p.(*208Gluext*39). Subsequent sequencing of the parents confirmed a de novo status of the variant.

Individual 3 was enrolled in the TIDEX study and trio exome sequencing at 3 years of age revealed a heterozygous de novo stop-loss variant in CLDN11 NM_005602.5:c.622T>C, p.(*208Glnext*39), the same as in Individual 1 (Tarailo-Graovac et al., 2016).

Sanger sequencing of index individuals, their parents and the unaffected brother of Individual 3 confirmed the identified variants and their de novo status.

Both variants c.622T>C, p.(*208Glnext*39) and c.622T>G, p.(*208Gluext*39) are not listed in more than 20 000 in-house exomes (Munich Exome Server) or in over 140 000 individuals of the Genome Aggregation Database (gnomAD v2.1.1; https://gnomad.broadinstitute.org/). The gnomAD does not list any stop-loss variants in CLDN11 (in v.2.1.1, or in v.3).

Table 1 Phenotype and genotype of the individuals

|	Individual 1 (German)	Individual 2 (Polish)	Individual 3 (Canadian)
Genetic and proband data			
Variant in CLDN11, chromosomal position (NC_000012.11, hg19)	chr3:g.170150542T > C	chr3:g.170150542T > G	chr3:g.170150542T > C
Variant in CLDN11, cDNA and protein position (NM_005602.5, NP_005593.2)	c.622T > C p.(*208Glnext*39)	c.622T > G p.(*208Gluext*39)	c.622T > C p.(*208Glnext*39)
Inheritance	De novo	De novo	De novo
Gender	Female	Male	Male
Ethnicity	Non-Finnish European (German; family from Germany)	Non-Finnish European (Polish; family from Poland)	Non-Finnish European (Canadian; maternal family from former Yugoslavia and Scotland, paternal family from Russia, Norway and Germany)
Age at last examination	13 years	8 years	6.5 years
Pyramid signs			
Babinski (yes/no)	+	+	+
Lower extremity tendon reflexes	++	+++	++
Axial/trunk muscle tone	Hypotonic	Rigid	Normal
Lower extremity muscle tone	High	High	High
Upper extremity muscle tone	High	High / rigid	Normal-high
Motor developmental milestones			
Sitting without support	Age 4.5 years	Age 3.5 years	Age 4 years
Walking without assistance	Few metres (at home)	Few metres age 5 years, lost ability to walk age 5.5 years	Never learned, stand shortly unsupported age 6 years
GMFCS level	III	III	III
Skeletal findings			
Scoliosis	–	–	–
Contractures	+	+	+
Other	Flat feet	Abnormal shoulder belt, short neck, concave chest	–
Mental development and speech			
Intelligence	Low-normal range	Low-normal range	Low-normal range
Autism	No	No	No
First words	2.2 years	4 years	2 years
Speech receptive	Good	Good	Good
Speech expressive	Simple sentences	Sentences up to 6 words	Sentences up to 6 words
Dysarticulation	Severe	Severe	Severe
Drooling	+	+	+
Visual system			
Nystagmus	+	+	+
Head nodding	–	–	+
Refraction error	Hypermetropia (+ 2.0 dpt) and astigmatism	Hypermetropia (+ 4.5/ + 4.25 dpt) and astigmatism	Hypermetropia (+ 3.25 dpt/ + 2.75 dpt) and astigmatism
Fundus	Normal	Normal	Normal (age 14 months) pale right optic disc (age 4 years)
Cataract	–	–	–
Strabism	+	+	+
Epilepsy			
EEG	Normal	Unspecific changes	Normal
Seizures	Single seizure at age 3 years, currently seizure-free without medication	No seizures	No seizures

+ / ++ / +++ /– = present (with graduation)/absent; GMFCS = gross motor function classification system.

Figure 2 features pedigrees of the three families and electropherograms of the stop-loss variant region of the three individuals and their parents (also of the unaffected brother of Individual 3).

RNA sequencing of cultivated skin fibroblasts (passage 3) of Individual 3 showed that the stop-loss variant has heterozygous expression on RNA level (Supplementary Fig. 1).
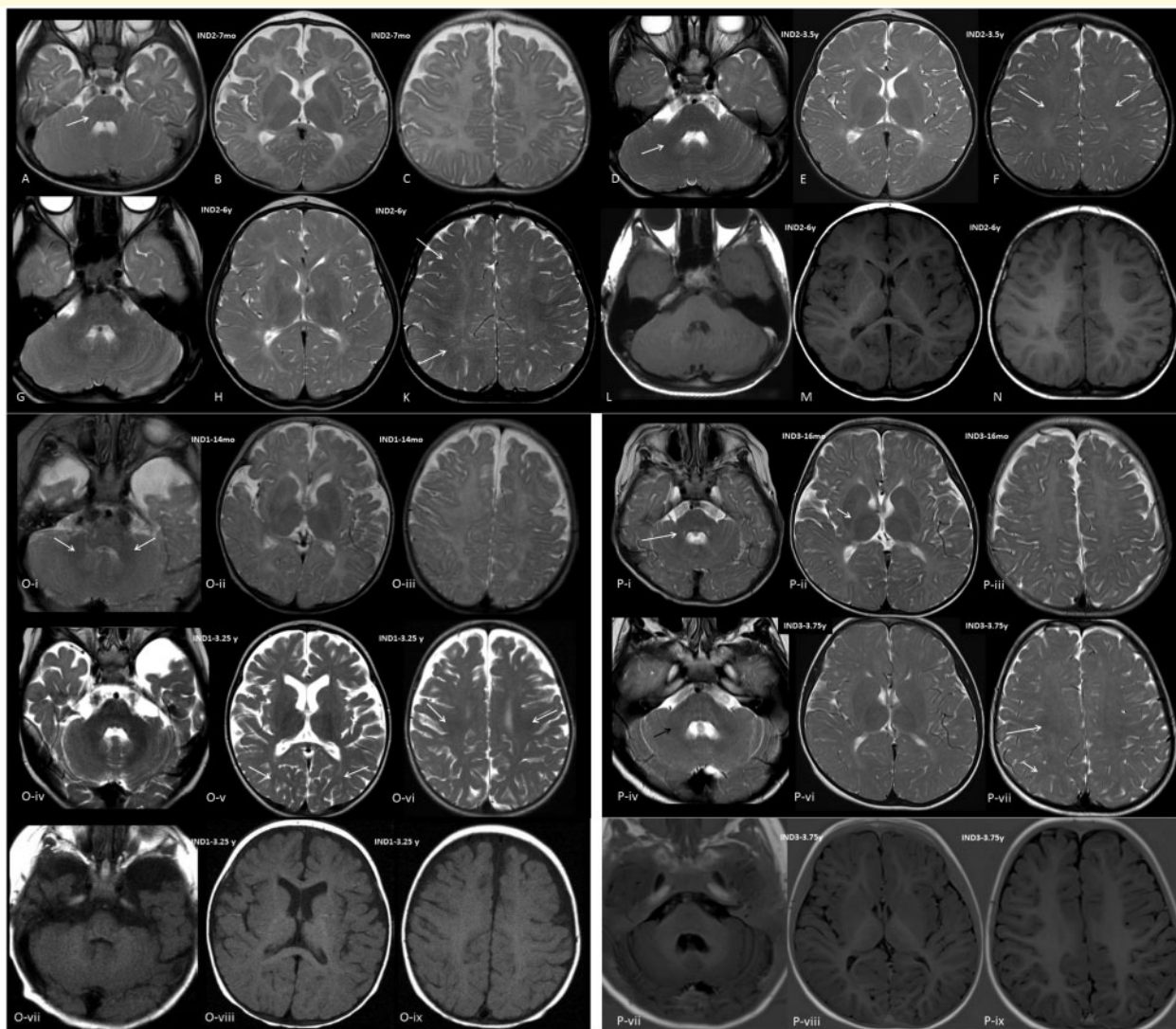
Figure 1 Cranial MRI images. Images shown are of Individual 2 (**A–N**), Individual 1 (**O**) and Individual 3 (**P**). (**A–C**) T_2-weighted axial images of Individual 2 at the age of 7 months, (**D–F**) T_2-weighted axial images at age 3.5 years, (**G–K**) T_2-weighted axial images, at age 6 years, and (**L–N**) T_1-weighted axial images at age 6 years at the level of the cerebellum (**A, D, G** and **L**), diencephalon (**B, E, H** and **M**) and centrum semiovale (**C, F, K** and **N**). There is no myelin equivalent at 7 months on T_2-weighted images except for a mildly lower signal in the cerebellar peduncles (arrow); at 3.5 years, central white matter shows some lower signal (arrows), as well as the central cerebellar white matter (short arrow); at 6 years, lower signal is seen in the more peripheral frontal and occipital white matter (arrows); T_1-weighted images at 6 years appear near normal, U-fibres are not clearly myelinated, however, and signal is slightly less hyperintense than normal. [**O(i–iii)**] T_2-weighted axial images of Individual 1 at the age of 14 months, (**iv–vi**) T_2-weighted axial images at age 3.25 years, (**vii–ix**) T_1-weighted images at age 3.25 years at the level of the cerebellum (**i, iv** and **vii**), diencephalon (**ii, v** and **viii**) and centrum semiovale (**iii, vi** and **ix**). There is no myelin equivalent at 14 months on T_2-weighted images except for a lower signal in the cerebellar peduncles (arrows) and cerebellar white matter, central white matter may show some minimally lower signal; at 3.25 years, central white matter shows lower signal (arrows), as well as the more peripheral occipital white matter (short arrows), the cerebellar white matter is clearly of low signal. T_1-weighted images at 3.25 years show hyperintensity of white matter with signal; however, less hyperintense than normal; U-fibres are not clearly myelinated. There is evidence of some global atrophy of the telencephalon (somewhat reduced white matter volume and enlarged sulci). [**P(i–iii)**] T_2-weighted axial images of Individual 3 at the age of 16 months, (**iv–vi**) T_2-weighted axial images and (**vii–ix**) Inversion recovery axial at age 3.75 years, at the level of the cerebellum (**i, iv** and **vii**), diencephalon (**ii, v** and **viii**) and centrum semiovale (**iii, vi** and **ix**). There is no myelin equivalent at 16 months on T_2-weighted except for a lower signal in the cerebellar peduncles and cerebellar white matter (arrow), and minimally in the posterior limb of the internal capsule (PLIC; short arrow); at 3.75 years, central white matter shows lower signal (arrow), as does the PLIC and the more peripheral occipital white matter (short arrow), the cerebellar white matter is clearly of low signal (black arrow); inversion recovery images at 3.75 years appear near normal, U-fibres are not clearly myelinated; however, as evident through the somewhat blurry differentiation between cortex and white matter; and signal is somewhat less hyperintense than normal. IND = individual; mo = months; y = years.
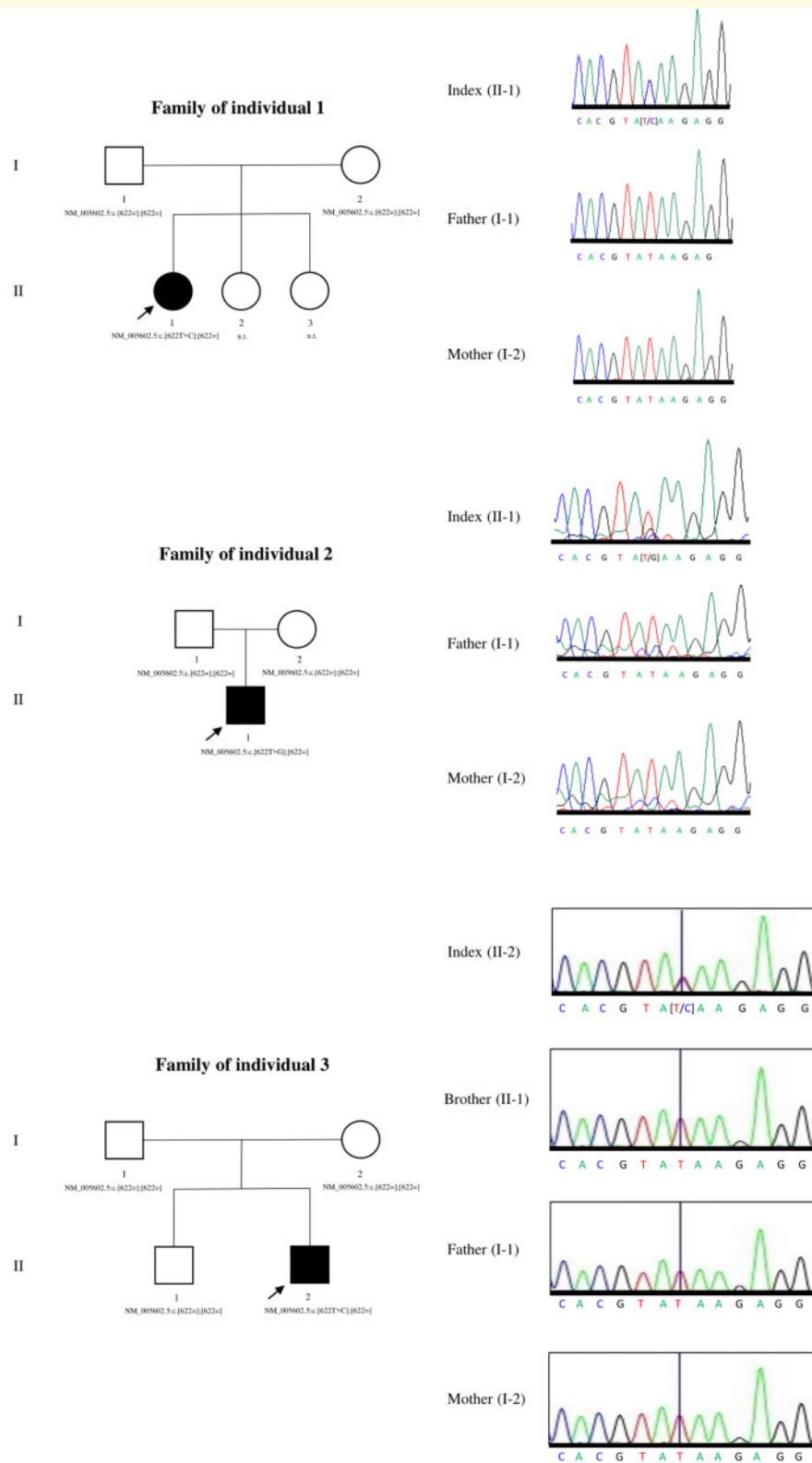
Figure 2 Pedigrees of the three families and electropherograms of the stop-loss variant region of the three individuals and their parents (also of the unaffected brother of Individual 3). Squares denote male individuals, circles denote female individuals.
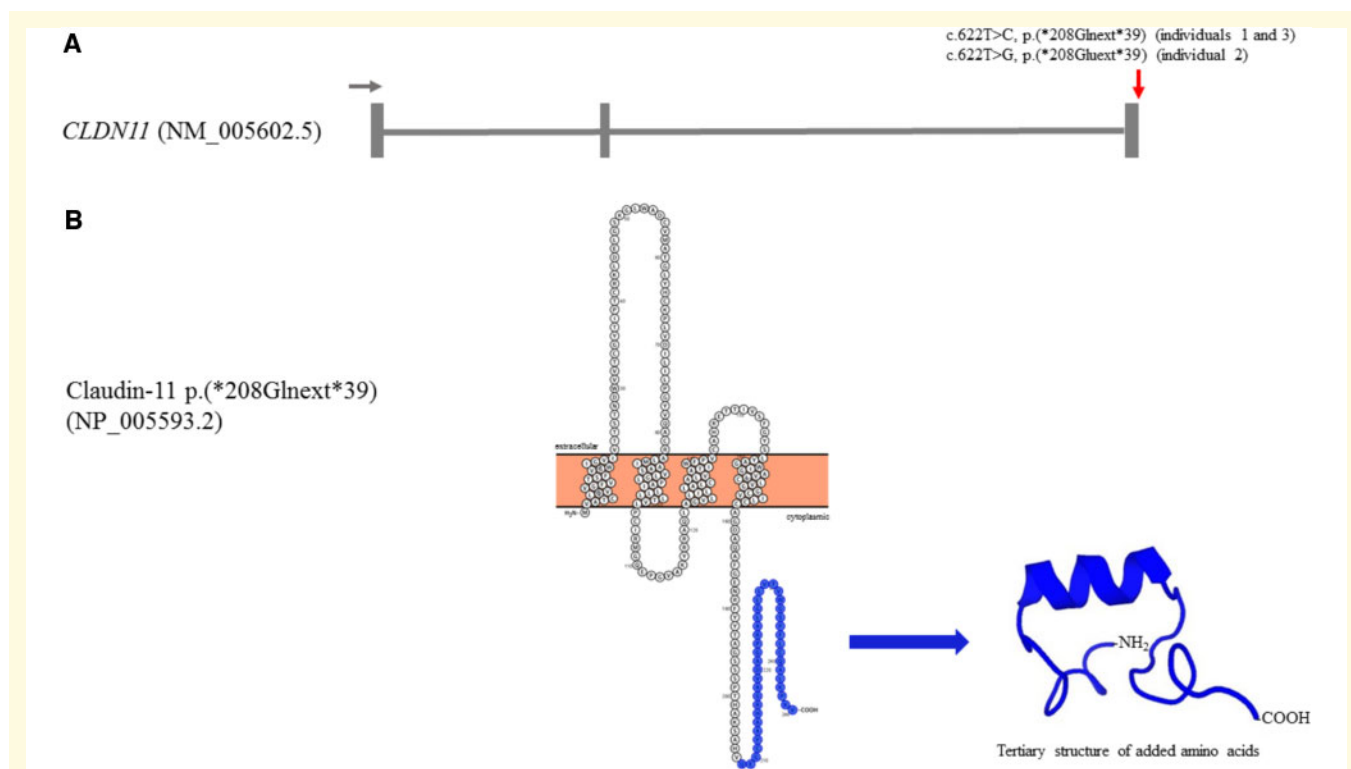
Figure 3 Gene structure and protein sequence/structure. (**A**) Gene structure of *CLDN11* featuring three exons (transcript NM_005602.5). Position of stop-loss variants is indicated by a red arrow (5′–3′ direction indicated by a grey arrow). (**B**) Protein sequence and tertiary structure of extended claudin-11. Added amino acids are depicted in blue in protein sequence [designed using the free web-based tool Protter (http://wlab.ethz.ch/protter/start/)]. Modelling of tertiary structure of added amino acids added was done with PEP-FOLD (Thevenet et al., 2012; Shen et al., 2014). Predicted tertiary structure of 39 added amino acid showing an alpha helix. All pertinent to variant NM_005602.5:c.622T > C, p.(*208Glnext*39) in *CLDN11* (individuals 1 and 3).

CLDN11 transcript expression levels are not significantly different from 156 control fibroblasts (Kremer *et al.*, 2017). Significantly downregulated genes (adjusted $P < 0.05$, fold change 0.5, 0.51, and 0.68, respectively) were *ESYT1*, *ZNF160*, and *DPM1* (Supplementary Table 1). The *ESYT1* expression level may be explained by the presence of a rare, heterozygous nonsense variant in *ESYT1* NM_015292.2:c.2956C > T, p.(Arg986*) in the individual's exome (inherited from the unaffected mother). *DPM1* is associated with an autosomal-recessive disease [congenital disorder of glycosylation, type Ie (MIM 608799)]. There is no direct interaction between *CLDN11*, *DPM1* and *ZNF160* (https://genemania.org/). *PLP1* is not expressed in fibroblasts (https://www.gtexportal.org/home/).

At the protein level, the *de novo* stop-loss variants are predicted to lead to an extension of 39 amino acids to the cytoplasmic C-terminus of claudin-11 and the added sequences (analysed for c.622T > C and c.622T > G) are unique as they do not have any significant similarity to any RefSeq protein sequence (Altschul *et al.*, 2005; Heinemann and Schuetz, 2019). The extension is predicted to add a domain with an alpha helix to the cytoplasmic tail of claudin-11 (computed by PEP-FOLD for variant c.622T > C) not incorporated into the cytoplasmic membrane (computed by TMHMM for

variant c.622T > C; see 'Materials and methods' section). Figure 3 illustrates the gene structure of *CLDN11* and protein structure of extended claudin-11.

Discussion

We present three unrelated individuals with hypomyelinating leukodystrophy, harbouring *de novo* stop-loss variants in *CLDN11* identified by exome sequencing, sharing strikingly overlapping genotypic and phenotypic characteristics.

Clinically, all three individuals had an early-onset phenotype, subsequently developed a spastic-rigid disorder without ataxia or dystonia, combined with a pronounced deficit in oral motor skills. Intellectual abilities were only mildly impaired.

Interestingly, all individuals had hypermetropia which has not been described in any other hypomyelinating leukodystrophy. This seems to be a noteworthy finding and might be a specific clinical sign of this hypomyelinating leukodystrophy, as is a high myopia in 4H leukodystrophy (Wolf *et al.*, 2005). However, it is certainly too early to call this an essential sign, since the prevalence of hyperopia in the general population is at least 6% at age 8–9 years (Donnelly *et al.*, 2005).

On cranial MRI, there was a discrepancy between T_1-weighted and T_2-weighted images, as described for hypomyelinating leukodystrophies, with lessening/absence of T_2-hypointensity without the significant lessening of T_1-hyperintensity seen in non-hypomyelinating leukodystrophies (Pouwels *et al.*, 2014). Signal intensity on T_1-weighted and inversion recovery images was higher than isointensity, but lower than considered normal for age, which indicated the presence of some myelin, and, thus, a moderate rather than severe myelin deficit. On T_2-weighted images, some progress in myelination with respect to central and peripheral white matter occurred which is not seen in classical PMD, for example (Plecko *et al.*, 2003). When clustering features of MRI in hypomyelinating disorders, Steenweg *et al.* (2010) did not describe such a feature as consistent in any disorder of their analysis. This feature, therefore, may help to draw attention to *CLDN11*.

CLDN11 encodes claudin-11, which has been identified as an indispensable protein in the formation of the radial component of myelin (Denninger *et al.*, 2015). After PLP (50–60% of myelin protein in CNS) and myelin basic protein (MBP, 40%), claudin-11 is the third most frequent protein in CNS myelin (7%) (Bronstein *et al.*, 1996, 1997). Knockout of *Cldn11* in mice leads to mild neurological deficits including body tremors and hindlimb weakness after birth, behavioural abnormalities and a reduction of nerve conduction. Interestingly, the absence of claudin-11 does not result in defective myelin formation underlining the role of claudin-11 in the physical properties but not integrity of myelin (Gow *et al.*, 1999; Devaux and Gow, 2008; Maheras *et al.*, 2018).

There is an association between *CLDN11* and *PLP1*; when both orthologues are absent in mice, a severe movement disorder develops with disruption of myelin formation and strong reduction in nerve conduction velocities. In contrast, knockout of either one of the genes does not lead to a substantial deficit in myelin. This might be because of compensatory effects as a knockout of one of the genes leads to upregulation of the other (Boison and Stoffel, 1994; Klugmann *et al.*, 1997; Gow *et al.*, 1999; Chow *et al.*, 2005). Interestingly, MBP, the second most abundant protein in CNS myelin after PLP is not differentially expressed when either or both *Plp1* or *Cldn11* are knocked out in mice, pointing towards the specific reciprocal regulation of *Plp1* and *Cldn11* (Chow *et al.*, 2005).

We identified the stop-loss variant c.622T>C, p.(*208Glnext*39) in two of the individuals and the stop-loss variant c.622T>G, p.(*208Gluext*39) in one individual in *CLDN11* (NM_005602.5). The genotypic data with three unrelated individuals with *de novo* stop-loss variants in *CLDN11* is very convincing since mutations of stop codons are rare events in human genetic disease [only 0.27% of 159 705 variants reported in the Human Gene Mutation Database (HGMD® Professional 2019.4)]. The variant c.622T>C, p.(*208Glnext*39) did not lead to a loss of *CLDN11* expression on RNA level in fibroblasts indicating this transcript is not subject to nonsense-mediated decay and most likely translated into an extended protein. As *PLP1* is not expressed in fibroblasts, our RNA sequencing data did not allow us to demonstrate a potential compensatory upregulation of *PLP1* expression in the presence of mutated *CLDN11*.

Both proteins claudin-11 and PLP1 are tetraspan integral membrane proteins of the myelin sheath (Devaux *et al.*, 2010). There is evidence that claudin-11 and PLP1 form complexes with integrins and further associated proteins in oligodendrocytes important for myelin proliferation and migration (Tiwari-Woodruff *et al.*, 2001; Gudz *et al.*, 2002). Importantly, claudin-11-associated protein 1 (OAP-1/tetraspanin 3; gene *TSPAN3*) forms a complex with claudin-11 and β1-integrin. For this, OAP-1 and claudin-11 interact via the C-terminus of claudin-11, which is heavily altered by the stop-loss variants identified in the three individuals (Bronstein *et al.*, 2000). Therefore, one possible mechanism could be that interaction of claudin-11 with OAP-1 (and β1-integrin and eventually PLP1) is disturbed by the added amino acids impairing myelinogenesis.

In conclusion, we describe three unrelated individuals with an autosomal dominant hypomyelinating leukodystrophy and a shared genotype of heterozygous *de novo* stop-loss variants in *CLDN11*. The consistent clinical phenotype and an MRI-pattern differing in part from classical PMD and other hypomyelinating disorders, may give guidance to the clinician.

Acknowledgements

Funding

Competing interests

The authors report no competing interests.

Supplementary material

Supplementary material is available at *Brain* online.

References

Altschul SF, Wootton JC, Gertz EM, Agarwala R, Morgulis A, Schaffer AA, et al. Protein database searches using compositionally adjusted substitution matrices. Febs J 2005; 272: 5101–9.

Boison D, Stoffel W. Disruption of the compacted myelin sheath of axons of the central nervous system in proteolipid protein-deficient mice. Proc Natl Acad Sci USA 1994; 91: 11709–13.

Bronstein JM, Chen K, Tiwari-Woodruff S, Kornblum HI. Developmental expression of OSP/claudin-11. J Neurosci Res 2000; 60: 284–90.

Bronstein JM, Micevych PE, Chen K. Oligodendrocyte-specific protein (OSP) is a major component of CNS myelin. J Neurosci Res 1997; 50: 713–20.

Bronstein JM, Popper P, Micevych PE, Farber DB. Isolation and characterization of a novel oligodendrocyte-specific protein. Neurology 1996; 47: 772–8.

Chow E, Mottahedeh J, Prins M, Ridder W, Nusinowitz S, Bronstein JM. Disrupted compaction of CNS myelin in an OSP/Claudin-11 and PLP/DM20 double knockout mouse. Mol Cell Neurosci 2005; 29: 405–13.

Denninger AR, Breglio A, Maheras KJ, LeDuc G, Cristiglio V, Deme B, et al. Claudin-11 tight junctions in myelin are a barrier to diffusion and lack strong adhesive properties. Biophys J 2015; 109: 1387–97.

Devaux J, Fykkolodziej B, Gow A. Claudin proteins and neuronal function. Curr Top Membr 2010; 65: 229–53.

Devaux J, Gow A. Tight junctions potentiate the insulative properties of small CNS myelinated axons. J Cell Biol 2008; 183: 909–21.

Donnelly UM, Stewart NM, Hollinger M. Prevalence and outcomes of childhood visual disorders. Ophthalmic Epidemiol 2005; 12: 243–50.

Gow A, Southwood CM, Li JS, Pariali M, Riordan GP, Brodie SE, et al. CNS myelin and sertoli cell tight junction strands are absent in Osp/claudin-11 null mice. Cell 1999; 99: 649–59.

Gudz TI, Schneider TE, Haas TA, Macklin WB. Myelin proteolipid protein forms a complex with integrins and may participate in integrin receptor signaling in oligodendrocytes. J Neurosci 2002; 22: 7398–407.

Heinemann U, Schuetz A. Structural features of tight-junction proteins. Int J Mol Sci 2019; 20:

Klugmann M, Schwab MH, Puhlhofer A, Schneider A, Zimmermann F, Griffiths IR, et al. Assembly of CNS myelin in the absence of proteolipid protein. Neuron 1997; 18: 59–70.

Kremer LS, Bader DM, Mertes C, Kopajtich R, Pichler G, Iuso A, et al. Genetic diagnosis of Mendelian disorders via RNA sequencing. Nat Commun 2017; 8: 15824.

Krogh A, Larsson B, von Heijne G, Sonnhammer EL. Predicting transmembrane protein topology with a hidden Markov model: application to complete genomes. J Mol Biol 2001; 305: 567–80.

Luders KA, Nessler S, Kusch K, Patzig J, Jung RB, Mobius W, et al. Maintenance of high proteolipid protein level in adult central nervous system myelin is required to preserve the integrity of myelin and axons. Glia 2019; 67: 634–49.

Maheras KJ, Peppi M, Ghoddoussi F, Galloway MP, Perrine SA, Gow A. Absence of claudin 11 in CNS myelin perturbs behavior and neurotransmitter levels in mice. Sci Rep 2018; 8: 3798.

Omasits U, Ahrens CH, Muller S, Wollscheid B. Protter: interactive protein feature visualization and integration with experimental proteomic data. Bioinformatics 2014; 30: 884–6.

Plecko B, Stockler-Ipsiroglu S, Gruber S, Mlynarik V, Moser E, Simbrunner J, et al. Degree of hypomyelination and magnetic resonance spectroscopy findings in patients with Pelizaeus Merzbacher phenotype. Neuropediatrics 2003; 34: 127–36.

Pouwels PJ, Vanderver A, Bernard G, Wolf NI, Dreha-Kulczewkski SF, Deoni SC, et al. Hypomyelinating leukodystrophies: translational research progress and prospects. Ann Neurol 2014; 76: 5–19.

Shen Y, Maupetit J, Derreumaux P, Tuffery P. Improved PEP-FOLD approach for peptide and miniprotein prediction. J Chem Theory Comput 2014; 10: 4745–58.

Steenweg ME, Vanderver A, Blaser S, Bizzi A, de Koning TJ, Mancini GM, et al. Magnetic resonance imaging pattern recognition in hypomyelinating disorders. Brain 2010; 133: 2971–82.

Tarailo-Graovac M, Shyr C, Ross CJ, Horvath GA, Salvarinova R, Ye XC, et al. Exome sequencing and the management of neurometabolic disorders. N Engl J Med 2016; 374: 2246–55.

Thevenet P, Shen Y, Maupetit J, Guyon F, Derreumaux P, Tuffery P. PEP-FOLD: an updated de novo prediction server for both linear and disulfide bonded cyclic peptides. Nucleic Acids Res 2012; 40: W288–93. (Web Server issue):

Tiwari-Woodruff SK, Buznikov AG, Vu TQ, Micevych PE, Chen K, Kornblum HI, et al. OSP/claudin-11 forms a complex with a novel member of the tetraspanin super family and beta1 integrin and regulates proliferation and migration of oligodendrocytes. J Cell Biol 2001; 153: 295–305.

van der Knaap MS, Bugiani M. Leukodystrophies - much more than just diseases of myelin. Nat Rev Neurol 2018; 14: 747–8.

van der Knaap MS, Schiffmann R, Mochel F, Wolf NI. Diagnosis, prognosis, and treatment of leukodystrophies. Lancet Neurol 2019; 18: 962–72.

Vanderver A, Prust M, Tonduti D, Mochel F, Hussey HM, Helman G, et al. Case definition and classification of leukodystrophies and leukoencephalopathies. Mol Genet Metab 2015; 114: 494–500.

Wolf NI, Harting I, Boltshauser E, Wiegand G, Koch MJ, Schmitt-Mechelke T, et al. Leukoencephalopathy with ataxia, hypodontia, and hypomyelination. Neurology 2005; 64: 1461–4.